

## Bureau International des Poids et Mesures

Comparison of the standards for absorbed dose to water  
of the ARPANSA and the BIPM for  $^{60}\text{Co}$  gamma radiation

P J Allisy-Roberts and D T Burns  
BIPM  
J F Boas, R B Huntley and K N Wise  
ARPANSA



October 2000

Pavillon de Breteuil, F-92312 SEVRES cedex

## **Comparison of the standards for absorbed dose to water of the ARPANSA and the BIPM for $^{60}\text{Co}$ gamma radiation**

by P J Allisy-Roberts and D T Burns  
Bureau International des Poids et Mesures, Sèvres

J F Boas, R B Huntley and K N Wise  
Australian Radiation Protection and Nuclear Safety Agency,  
Lower Plenty Road, Yallambie, Victoria 3085, Australia

### **Abstract**

A comparison of the standards for absorbed dose to water of the Australian Radiation Protection and Nuclear Safety Agency and of the Bureau International des Poids et Mesures (BIPM) has been carried out in  $^{60}\text{Co}$  gamma radiation. The Australian standard is based on a graphite calorimeter and the subsequent conversion from absorbed dose to graphite to absorbed dose to water using the photon fluence scaling theorem. The BIPM standard is ionometric using a graphite-walled cavity ionization chamber. The comparison result is 1.0024 (standard uncertainty 0.0029).

### **1. Introduction**

An indirect comparison of the standards of absorbed dose to water of the Australian Radiation Protection and Nuclear Safety Agency (ARPANSA), Victoria, Australia and of the Bureau International des Poids et Mesures (BIPM) was carried out in  $^{60}\text{Co}$  gamma radiation.

The Australian primary standard for absorbed dose is a graphite calorimeter as described in [1] and [2], the absorbed dose to water for  $^{60}\text{Co}$  radiation being derived from the absorbed dose to graphite using the photon fluence scaling theorem. The BIPM primary standard is a graphite cavity ionization chamber of pancake geometry as described in [3]. This absorbed dose to water comparison is the first such comparison made between the two laboratories.

The comparison was undertaken using two ionization chambers belonging to the ARPANSA as transfer standards. The chambers were calibrated at the ARPANSA before and after the measurements made at the BIPM in April 1997. The result of the comparison is derived from the ratios of the calibration factors of the transfer chambers determined at the two laboratories.

## 2. Determination of absorbed dose to water

### 2.1 The BIPM standard

At the BIPM, the absorbed dose rate to water is determined from

$$\dot{D}_{w,BIPM} = (I/m)(W/e)\bar{s}_{c,a}\Psi_{w,c}(\bar{\mu}_{en}/\rho)_{w,c}(1+\varepsilon)_{w,c}\Pi k_i, \quad (1)$$

where

- $I/m$  is the mass ionization current measured by the standard,
- $W$  is the mean energy expended in dry air per ion pair formed,
- $e$  is the electronic charge
- $\bar{s}_{c,a}$  is the ratio of the mean mass stopping powers of graphite and air,
- $\Psi_{w,c}$  is the ratio of the photon energy fluence in water and graphite at the reference point in the water phantom,
- $(\bar{\mu}_{en}/\rho)_{w,c}$  is the ratio of the mean mass energy-absorption coefficient for water to that in graphite averaged over the unperturbed and perturbed photon spectrum at the reference point,
- $(1+\varepsilon)_{w,c}$  is the ratio of the absorbed dose to the collision component of kerma, at the reference point in water to the same ratio at the reference point in graphite, and
- $\Pi k_i$  is the product of the other correction factors to be applied to the standard.

The ionometric method is described fully in [3], which also gives the values of the physical constants and the correction factors  $k_i$  for the BIPM standard together with their uncertainties. The combined relative standard uncertainty in the absorbed dose is  $2.9 \times 10^{-3}$ , the detailed uncertainty budget being given in Table 1 of this report.

Absorbed dose is determined at the BIPM under the reference conditions defined by the Consultative Committee for Ionizing Radiation (CCRI, previously the CCEMRI) [4]:

- the distance from the source to the reference plane (the centre of the detector) is 1 m;
- the field size in air at the reference plane is 10 cm  $\times$  10 cm, the photon fluence rate at the centre of each side of the square being 50 % of the photon fluence rate at the centre of the square;
- the reference depth in water is 5 g cm<sup>-2</sup>.

**Table 1. Physical constants, correction factors and relative standard uncertainties for the BIPM ionometric standard for absorbed dose to water**

Quantity	BIPM value	BIPM relative standard uncertainty <sup>(1)</sup>	
		100 $u_i$ ; ( $\nu_i$ )	100 $u_j$
Dry air density <sup>(2)</sup> / (kg m <sup>-3</sup> )	1.293 0	–	0.01
$W/e$ / (J C <sup>-1</sup> )	33.97	–	0.11 <sup>(3)</sup>
$\bar{s}_{c,a}$	1.003 0	–	
$k_{cav}$ (air cavity)	0.990 0	0.03	0.04
$(\bar{\mu}_{en}/\rho)_{w,c}$	1.112 5	0.01	0.14
$\Psi_{w,c}$ (photon fluence ratio)	1.006 5	0.04	0.06
$(1+\varepsilon)_{w,c}$ (dose to kerma ratio)	1.001 5	–	0.06
$k_{ps}$ (PMMA envelope)	0.999 9	<0.01	0.01
$k_{pf}$ (phantom window)	0.999 6	–	0.01
$k_{rn}$ (radial non-uniformity)	1.005 1	<0.01	0.03
$k_s$ (recombination losses)	1.001 6	<0.01	0.01
$k_h$ (humidity)	0.997 0	–	0.03
Volume <sup>(4)</sup> /cm <sup>3</sup>	6.881 0	0.19	0.03
$I$ (ionization current)	–	0.01 ; (7)	0.02
Quadratic summation		0.20	0.21
Combined relative standard uncertainty of $D_{w,BIPM}$		0.29	

- (1) In Tables 1 to 3 and 8,  $u_i$  represents the Type A relative standard uncertainty  $u_A(x_i)/\bar{x}_i$  estimated by statistical means;  $\nu_i$  represents the number of degrees of freedom;  $u_j$  represents the Type B relative standard uncertainty  $u_B(x_j)/\bar{x}_j$  estimated by other means.
- (2) At 0 °C and 101.325 kPa.
- (3) Combined uncertainty for the product of  $(W/e)\bar{s}_{c,a}$
- (4) Using standard chamber serial number CH4-1.

## 2.2 The ARPANSA standard

### 2.2.1 Method of measurement

At the ARPANSA the absorbed dose to water is derived from the calorimetric determination of the absorbed dose to graphite by the relation

$$D_{w,ARPANSA} = D_c \Psi_c^w (\bar{\mu}_{en}/\rho)_c^w \beta_c^w \Pi k_i, \quad (2)$$

where

$D_c$  is the absorbed dose to graphite at the reference point in graphite,

$\Psi_c^w$  is the ratio of the photon energy fluence at the reference points in water and graphite,<sup>1</sup>

$(\bar{\mu}_{en}/\rho)_c^w$  is the ratio of the mean mass energy-absorption coefficients for water and graphite for the photon energy spectra at the corresponding reference points,<sup>1</sup>

$\beta_c^w = \beta_w / \beta_c$  where  $\beta$  is the ratio of the absorbed dose to the collision component of kerma, at the reference point<sup>1</sup> in water (w) or in graphite (c), and

$\Pi k_i$  is the product of the correction factors to be applied to the standard.

The factors  $(\bar{\mu}_{en}/\rho)_c^w$  and  $\beta_c^w$  are derived by calculation [5], and the photon fluence ratio  $\Psi_c^w$  is determined using the "dose ratio" method [6, 7] as described in section 2.2.3.

Absorbed dose to water is determined at the ARPANSA under the following reference conditions which are slightly different from those at the BIPM:

- the distance from the source to the surface of the water phantom is 1 m;
- the field size at the reference plane (nominally 1.05 m from the source) is 10.5 cm × 10.5 cm;
- the reference depth in water is 5 g cm<sup>-2</sup>.

### 2.2.2 Determination of absorbed dose to graphite at the ARPANSA

The ARPANSA standard of absorbed dose to graphite is a Domen-type calorimeter [8] constructed by the Österreichisches Forschungszentrum Seibersdorf (ÖFZS) as described by Witzani et al. [9]. The absorbed dose rate to graphite,  $\dot{D}_c$ , at the reference point in graphite is given by

$$\dot{D}_c = (P/m) k_{\text{gap}} k_z k_m k_{\text{an}} k_t. \quad (3)$$

<sup>1</sup> The different notation compared with that of equation (1) reflects the different experimental arrangements at the BIPM and at the ARPANSA.

The physical quantities and correction factors in equation (3) are as described below and are listed with their relative standard uncertainties in Table 2.

**Table 2. Physical quantities, correction factors and relative standard uncertainties for the determination of absorbed dose to graphite at the ARPANSA**

Quantity	ARPANSA value	ARPANSA relative standard uncertainty	
		100 $s_i$ ; ( $v_i$ )	100 $u_i$
$P$ (power calculation)	–	0.08 ; (152)	0.04
Repeatability	–	0.05 ; (13)	
$m$ (core mass) /g	1.5622		0.01
$k_{\text{gap}}$ (calorimeter gaps)	1.0074	<0.01	0.04
$k_z$ (graphite depth)	0.9934	0.01 ; (4)	0.03
$k_{\text{rn}}$ (radial non-uniformity)	1.0026	0.02 ; (80)	0.04
$k_{\text{an}}$ (axial non-uniformity)	1.0000	<0.01 ; (5)	0.05
$k_t$ (source decay)	–		0.01
Quadratic summation		0.10	0.09
Combined relative standard uncertainty of $D_c$		0.13	

*The radiation power absorbed in the graphite core,  $P$*

This is calculated [1, 2] from voltage and resistance measurements. The calorimeter is normally operated in the quasi-isothermal mode [9] in which the electrical power input to the calorimeter core in the absence of radiation is matched as closely as possible to the anticipated radiation power. The electric heating is switched off at the same time as the radiation source is switched on, so that the rate of heating of the core remains approximately constant. The radiation power input can thus be determined readily against the ARPANSA working standards of resistance and voltage.

*The mass of the calorimeter core,  $m$*

This was measured at the ÖFZS and corrected for impurities and buoyancy.

*Correction factor for the calorimeter gaps,  $k_{\text{gap}}$*

The difference between the absorbed dose rate at the centre of the calorimeter core and that at the same position in a solid graphite phantom is calculated using Monte-Carlo codes [5] and the correction factor,  $k_{\text{gap}}$ , is derived from these results. The ARPANSA gap correction is calculated for a 35 mm radius field (cross-section approximately equivalent to a 65 mm × 65 mm field) incident on the calorimeter with the centre of the core at a depth in graphite of 30 mm ( $5.37 \text{ g cm}^{-2}$ ) and at a distance of 650 mm from the source.

*Correction factor for the reference depth in graphite,  $k_z$* 

The desired reference depth is not achieved exactly with the available combination of graphite build-up plates. Thus a correction is applied which is obtained by interpolation from attenuation measurements.

*Correction factor for radial non-uniformity of the  $^{60}\text{Co}$  beam over the calorimeter core,  $k_{rn}$* 

This was obtained experimentally by measuring the radial profile of the beam using an NE 2561 thimble ionization chamber.

*Correction for the axial non-uniformity of the  $^{60}\text{Co}$  beam over the calorimeter core,  $k_{an}$* 

This was obtained from the departure from linearity of the measured depth-dose distribution over the calorimeter core.

*Normalization factor for the reference date and time,  $k_t$* 

The calorimeter measurements were corrected to the reference date and time of 1997-03-15 at 12:00 Australian Eastern Daylight Time<sup>2</sup>. The half life of  $^{60}\text{Co}$  was taken as 1 925.5 d,  $\sigma = 0.5$  d [10].

### 2.2.3 Conversion of absorbed dose to graphite into absorbed dose to water by the "dose ratio" method at the ARPANSA

In the "dose ratio" method, the photon fluence scaling theorem [11] is used to determine  $\Psi_c^w$  for a point source of radiation by scaling the phantom dimensions, measurement depths and distances from the source in the inverse ratio (0.619 58) of the electron densities of water and the graphite (using the tabulated value of water density at 20 °C, 0.998 22 g cm<sup>-3</sup>, the measured graphite bulk density, 1.790 g cm<sup>-3</sup>, and the  $Z/A$  ratios). Under these conditions and assuming that Compton scattering is the only interaction mechanism, the ratio of primary to scattered radiation energy fluences will be the same at corresponding points, i.e. the energy spectra will have the same shape. Furthermore, the ratio of the primary photon energy fluences at these mapped reference points will be in the inverse ratio of the square of their distances from the source:

$$\Psi_c^w = (r_c/r_w)^2 k_{pg} k_{nc}, \quad (4)$$

where  $r_c$  and  $r_w$  are the distances from the source to the reference points in graphite and water respectively, and  $k_{pg} k_{nc}$  are corrections needed for failure to completely satisfy the requirements of the photon fluence scaling theorem as explained in the following paragraphs.

<sup>2</sup> AEDT = UCT + 11 h, where AEDT is Australian Eastern Daylight Time and UCT is Universal Coordinated Time

*Distances from the source to the reference points in graphite and water,  $r_c$  and  $r_w$* 

The position of the source centre was approximated by application of the inverse square law to ionization chamber current measurements in air along the beam axis, corrected for air attenuation, as described by Wise [5]. The distance from the source to the reference point in water is fixed by the reference conditions at 1.050 m, and from the scaling theorem, the distance to the reference point in graphite is 650.56 mm. The uncertainty in the graphite density of  $0.005 \text{ g cm}^{-3}$  leads to an uncertainty in the scaled graphite reference distance of 1.82 mm. The scaled reference depth in graphite is  $(31.03 \pm 0.09)$  mm. The components of the uncertainty in  $(r_c/r_w)^2$  are considered in [1] and include contributions from the water phantom which also enter into the uncertainty in the water-depth correction for the transfer chamber.

*Correction factors for the limitations of the photon fluence scaling theorem as applied to the graphite and water phantoms,  $k_{pg}$  and  $k_{nc}$* 

The factor  $k_{pg}$  corrects for the failure to scale the graphite phantom geometry to that of the water phantom. The factor  $k_{nc}$  corrects for the small number of non-Compton interactions which are not proportional to the electron density. These factors have been evaluated by Wise [5] using Monte-Carlo simulations with correlated sampling.

Thus  $D_w$  can be calculated from  $D_c$  provided that  $r_c$ ,  $r_w$ ,  $k_{pg}$ ,  $k_{nc}$  and the physical quantities in (2) and (3) are known. In practice, two additional corrections are applied and the absorbed dose to water at the reference point is given by

$$D_{w,ARPANSA} = D_c \Psi_c^w (\bar{\mu}_{en}/\rho)_c^w \beta_c^w k_{win} k_{air}. \quad (5)$$

The physical quantities and the correction factors  $k_{win}$  and  $k_{air}$  are described below and are listed in Table 3 together with their relative standard uncertainties.

*Ratios of mass energy-absorption coefficients  $(\bar{\mu}_{en}/\rho)_c^w$  and of the quotients of absorbed dose to the collision component of kerma,  $\beta_c^w$* 

These were obtained using published data for the coefficients [12] and Monte-Carlo simulations of the energy spectra at the reference points in the water and graphite phantoms as described by Wise [5].

*Correction factor for the difference in attenuation of the front window of the water phantom and that of the same thickness of water,  $k_{win}$* 

For the ARPANSA water phantom used for measurements with  $^{60}\text{Co}$  radiation, the beam passes through a PMMA<sup>3</sup> window of thickness 2 mm and the correction factor was evaluated theoretically [5].

*Correction factor for air attenuation over the distance between the graphite calorimeter and the water phantom,  $k_{air}$* 

This was derived from the simulated energy spectrum of the radiation beam and the attenuation coefficients of air [12] at the appropriate energies.

---

<sup>3</sup> Polymethylmethacrylate

**Table 3. Physical quantities, correction factors and relative standard uncertainties for conversion of absorbed dose to graphite to absorbed dose to water by the "dose ratio" method**

Quantity	ARPANSA value	ARPANSA relative standard uncertainty	
		100 $u_i$ ( $v_i$ )	100 $u_i$
$D_c$ (see Table 2)	–	0.10	0.09
$(r_c/r_w)^2$	0.383 88	–	0.05
$k_{nc}$ (non-Compton interactions)	0.9996	<0.01	0.02
$k_{pg}$ (phantom geometry)	0.9998	<0.01	0.02
$(\bar{\mu}_{en}/\rho)_c^w$	1.1131	0.01	0.14
$\beta_{w,c}$ (dose to kerma ratio)	1.0003	<0.01	<0.01
$k_{win}$ (water equivalence)	0.9988	–	0.03
$k_{air}$ (attenuation)	0.9972	–	0.01
Quadratic summation		0.10	0.18
Combined relative standard uncertainty of $D_{w,ARPANSA}$		0.20	

### 3. Procedure for the comparison

#### 3.1 The use of transfer chambers

The comparison of the ARPANSA and BIPM standards was made indirectly by means of the calibration factors  $N_{Dw}$  for the ARPANSA transfer chambers given by

$$N_{Dw,lab} = \dot{D}_{w,lab} / I_{lab} \quad (6)$$

where  $\dot{D}_{w,lab}$  is the absorbed dose rate to water and  $I_{lab}$  is the ionization current of a transfer chamber normalized to the same reference date, each measured at the ARPANSA or the BIPM. Current measurements are corrected for the effects and influences described in this section.

The  $\dot{D}_{w,BIPM}$  value is the mean of measurements performed at the BIPM under the reference conditions over a period of three months before and after this comparison. By convention it is given at the reference date of 1997-01-01, 0:00 UCT, as is the value of  $I_{BIPM}$  (The value for the half life of  $^{60}\text{Co}$  recommended by the IAEA [10] is used at both laboratories). The relative standard uncertainty of the mean of these eight measurements is  $10^{-4}$ .

The  $\dot{D}_{w,ARPANSA}$  value is derived from the mean of 14 calorimeter measurements made since the installation of a new  $^{60}\text{Co}$  source at the ARPANSA in March 1995 and corrected to a

reference date of 1997-03-15 at 12:00 AEDT. The relative standard uncertainty of the distribution of these 14 measurements is  $4.5 \cdot 10^{-4}$ . The ionization chamber currents are the mean of measurements made before and after the measurements at the BIPM, normalized to the same reference date and time.

The two laboratories determine absorbed dose by methods that are quite different and the only significant correlation is that due to the use of  $(\bar{\mu}_{\text{en}}/\rho)_{\text{w,c}}$  or  $(\bar{\mu}_{\text{en}}/\rho)_{\text{c}}^{\text{w}}$ . Note that these ratios are slightly different but are assumed to be fully correlated. The uncertainty of the result of the comparison is obtained by summing in quadrature the remaining uncorrelated uncertainties of  $\dot{D}_{\text{w,BIPM}}$ ,  $\dot{D}_{\text{w,ARPANSA}}$  and the contributions arising from the use of transfer standards. The ARPANSA transfer standards used for this comparison are graphite cavity ionization chambers manufactured by Nuclear Enterprises (Type NE 2561, serial numbers 070 and 328). Their main characteristics are listed in Table 4.

**Table 4. Characteristics of the transfer chambers type NE 2561**

Characteristic		Serial numbers 070 and 328
Dimensions	Inner diameter / mm	7.35
	Wall thickness / mm	0.5
	Cavity length / mm	9.22
	Cavity centre from tip / mm	5.00
Electrode	Diameter / mm	1.00
Volume	Air cavity / cm <sup>3</sup>	0.325
Wall	Material	graphite < 0.01% impurity
	Density / (g cm <sup>-3</sup> )	1.80
Build-up cap	Material	Delrin
	Thickness / mm	3.87
Applied voltage	Negative polarity / V	210

The calibration procedures are described briefly below and are discussed in more detail in [1, 2] and [13] for the ARPANSA and the BIPM, respectively.

### 3.2 Measurement conditions and corrections

The ARPANSA water phantom is a cube of side length 300 mm, with a wall thickness of 12 mm except for the beam entrance window which is a 60 mm diameter circle of thickness 2 mm. The BIPM phantom is a cube of similar size with a square window of side length 150 mm and 4 mm thick.

#### *Positioning of transfer chambers in the water phantoms*

At the ARPANSA, the depth of the centre of the transfer chamber was adjusted to 50 mm (standard uncertainty 0.05 mm) using a depth gauge and a computerized motion control system; this distance includes the front window of the phantom. The ionization current is corrected to a depth of 5 g cm<sup>-2</sup> using tabulated depth dose data [14] which give a relative

gradient of  $4 \times 10^{-3} \text{ mm}^{-1}$ . At the BIPM, the centre of the transfer chamber is placed at  $5 \text{ g cm}^{-2}$  accounting for the window (its thickness and density, its distortion due to the water pressure and its non-equivalence to water in terms of interaction coefficients) and for the water density at its measured temperature, and so no correction is required for depth. In each laboratory, any small difference (not more than 1 mm) between the reference distance (1 m and 1.05 m for the BIPM and ARPANSA respectively) and the distance at which the measurement is made, is corrected by the inverse square law.

#### *Waterproof sleeve*

Each chamber was supplied with a thin-walled (0.5 mm) PMMA waterproof sleeve manufactured at the ARPANSA. At the ARPANSA, a correction factor of 1.0003 is applied to the current measured using the transfer chamber in the water phantom to account for the increased attenuation of the PMMA sleeve over that of the same thickness of water. For consistency the same correction was applied to the measurements of current at the BIPM.

#### *Humidity, temperature and pressure*

During calibration, the relative humidity at the BIPM was between 48 % and 52 %; the air temperature was around 21 °C and was stable to better than 0.01 °C during a series of measurements. At the ARPANSA the relative humidity can vary between 30 % and 90 %; the temperature was around 23 °C and was stable to within 0.02 °C during a series of measurements. At both laboratories, the temperature of an air cavity in the water phantom is measured with a calibrated thermistor. The measured ionization current is normalized to a temperature of 293.15 K and a pressure of 101.325 kPa, as part of each laboratory's measurement system. At the ARPANSA, corrections of between 0.02 % and 0.09 % (standard uncertainty 0.01 %) were made to correct the results to 50 % relative humidity. These corrections were calculated from an empirical fit, as described in [1, 2]. No such correction is required at the BIPM as humidity is closely controlled.

#### *Collecting voltage*

A collecting voltage of 210 V (negative polarity) was supplied at each laboratory. The collecting voltage was applied at the BIPM for at least 30 minutes before measurements were made. At the ARPANSA, measurement results showing an initial drift were excluded.

#### *Measurement of charge*

The charge  $Q$  collected by the chambers was measured using the local measurement system at the BIPM and at the ARPANSA. The chambers were irradiated for at least 30 minutes before measurements commenced at the BIPM. The measured current was corrected at the BIPM for the leakage current of about 0.02 %. No correction was made for this at the ARPANSA, as the combined effect of background, leakage and bias current was typically less than 0.01 %. The uncertainty due to this is included in the uncertainty for ionization chamber measurements. To detect any gross changes in the transfer chambers during transport, a check source of  $^{90}\text{Sr}$  belonging to the ARPANSA (NE2562, serial number 024) was used to irradiate the chambers in a constant geometry. The consequent ionization currents measured at both the ARPANSA and the BIPM were normalized for temperature and pressure, to 50 % relative humidity as described above, and for radioactive decay to a common reference date of 1997-03-15. The half life of  $^{90}\text{Sr}$  was taken as 28.8 years. The mean result for the two chambers, expressed as a current ratio  $R_I = I_{\text{ARPANSA}} / I_{\text{BIPM}}$ , was 1.0010 [15]. As discussed in [1, 2], variations within a range of about 0.3 % have been noted for  $^{90}\text{Sr}$  measurements with the NE2561 chambers at

the ARPANSA. At this level of uncertainty, no changes due to transport were observed and no difference between the measurement systems of the two laboratories could be identified.

#### *Recombination and polarity*

The value of the recombination correction factor for the NE 2561 chambers measured and applied at the ARPANSA is 1.0017 [1, 2]. For consistency, as initial recombination predominates and is independent of the dose rate, the same value was applied at the BIPM, the measurement conditions being similar. The transfer chambers were used with negative polarity at both laboratories and no correction factor was applied for the polarity effect.

#### *Radial non-uniformity*

No correction to the measurements was made at either the ARPANSA or the BIPM for the radial non-uniformity of the beam over the cross-section of the sensitive volume of the transfer chambers. For NE 2561 chambers this effect is less than 0.02 % at each laboratory.

The transfer chamber correction factors and their associated uncertainties are summarized in Table 5.

**Table 5. Corrections and combined relative standard uncertainties for transfer chamber measurements at the ARPANSA and at the BIPM in their respective water phantoms**

Measurement	Value applied at the ARPANSA and the BIPM	Relative standard uncertainty 100 $u_c/x$		Combined uncertainty <sup>(1)</sup> of the ratio
		ARPANSA	BIPM	$I_{\text{BIPM}}/I_{\text{ARPANSA}}$
Reference distance	-	0.01	0.02	0.02
Depth position and correction	0.9996 <sup>(2)</sup>	0.03	0.02	0.04
Waterproof sleeve	1.0003	0.01	0.01	–
Temperature, pressure and humidity corrections	–	0.03	0.02	0.04
Charge measurement	–	0.03	0.02	0.04
Recombination	1.0017	0.03	0.03	–
Radial non-uniformity	1	0.01	0.01	0.01
Decay correction	–	0.01	–	0.01
Combined relative standard uncertainty		0.06	0.05	0.07

(1) Uncertainties of the correlated values have been removed.

(2) At the ARPANSA, the correction shown is to the reference depth of 5 g cm<sup>-2</sup>, the combined uncertainty arises from the actual depth set using the gauge (0.02 %), the front window thickness (0.02 %) and the ambient water temperature, 17 °C to 23 °C (0.01 %). At the BIPM the chamber is placed at the reference depth so no correction is needed; the combined uncertainty arises from the phantom window, the water density correction and the depth position measurement uncertainty.

#### 4. Results of the comparison

##### *Reproducibility of measurements*

The short-term relative standard deviation of the mean ionization current, measured by each transfer chamber, was  $3 \times 10^{-4}$  at the ARPANSA (three series each of 50 measurements of 400 pC for each chamber) and  $2 \times 10^{-4}$  at the BIPM (four series each of 30 measurements of 1000 pC for each chamber). The differences in the currents using the  $^{90}\text{Sr}$  check source measured by the ARPANSA before and after calibration at the BIPM are compatible with these short-term variations as shown in Table 6.

**Table 6. Stability of the ARPANSA transfer chambers and check source measurements**

Date	$I_{\text{Sr, ARPANSA, 1997-03-15}} / \text{pA}$		Ratio
	Chamber 070	Chamber 328	070/328
March 1997	23.681	22.645	1.0457
May/June 1997	23.703	22.660	1.0460
Relative difference	+0.09 %	+0.07 %	+0.03 %

Table 7 gives the relevant values for the calculation of  $N_{D,w}$  using (6), and the results of the comparison,  $R_{Dw}$ , expressed in the form

$$R_{Dw} = N_{Dw, \text{ARPANSA}} / N_{Dw, \text{BIPM}} \quad (7)$$

In the stated uncertainty  $u_c$  of  $R_{Dw}$ , the correlated uncertainties arising from the use of transfer chambers and from  $(\bar{\mu}_{\text{en}}/\rho)_{w,c}$  have been removed. Table 8 summarizes the uncertainty components.

The comparison result, 1.0024, is taken from the mean value for both transfer chambers, with a combined standard uncertainty of 0.0029. The difference ( $3 \times 10^{-4}$ ) between the results  $R_{Dw}$  for the two chambers is compatible with the statistical uncertainty ( $4 \times 10^{-4}$ ) of the charge measurements.

**Table 7. Calibration factors and the results of the comparison**

Transfer chamber	$\dot{D}_{w, \text{ARPANSA}} / (\text{mGy s}^{-1})$	$I_{\text{ARPANSA}} / \text{pA}$	$N_{Dw, \text{ARPANSA}} / (\text{Gy } \mu\text{C}^{-1})$	$\dot{D}_{w, \text{BIPM}} / (\text{mGy s}^{-1})$	$I_{\text{BIPM}} / \text{pA}$	$N_{Dw, \text{BIPM}} / (\text{Gy } \mu\text{C}^{-1})$	$R_{Dw}$	$u_c$
NE2561 070	4.679	45.751	102.27	4.617	45.260	102.01	1.0025	0.0029
NE2561 328	4.679	45.397	103.07	4.617	44.896	102.84	1.0022	0.0029
mean values							1.0024	0.0029

**Table 8. Estimated relative standard uncertainties of the calibration factor,  $N_{Dw}$ , of the transfer chambers and of  $R_{Dw}$** 

Quantity	Relative standard uncertainty				Combined uncertainty of $R_{Dw}$	
	ARPANSA		BIPM			
	100 $u_i$	100 $u_j$	100 $u_i$	100 $u_j$	100 $u_i$	100 $u_j$
Absorbed dose rate to water (Tables 1 and 3)	0.10	0.18	0.20	0.21	0.22	0.18
Transfer chamber measurements (Table 5)	0.06		0.05		0.07	
<b>Relative standard uncertainties of <math>N_{Dw,lab}</math></b>	0.21		0.29		–	
<b>Relative standard uncertainty of <math>R_{Dw}</math></b>	–		–		0.29	

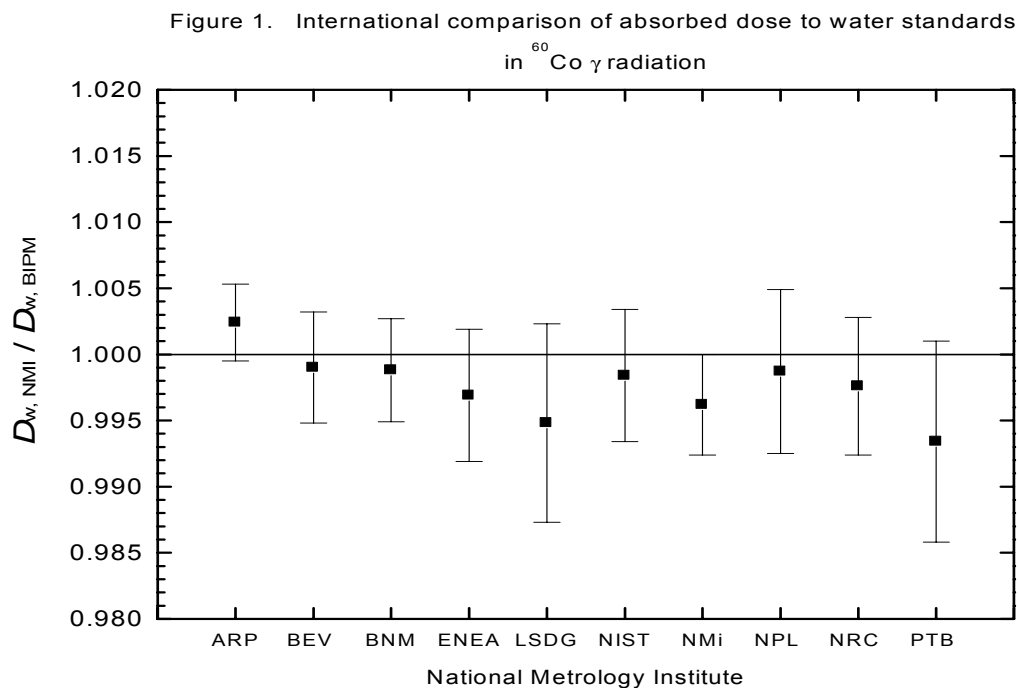
The two transfer chambers were also used in a concurrent comparison of air kerma standards [15], from which the result was  $R_K = 1.0028$ . Consequently it is possible to obtain the ratio  $N_{Dw}/N_K$ , as shown in Table 9, to check the consistency of the chambers. The values obtained at each laboratory, corrected for the factors described in this report, reflect the consistency of the chambers ( $3 \times 10^{-4}$ ), and the difference between the ARPANSA and the BIPM values ( $3 \times 10^{-4}$ ) reflects the difference in the comparison results for absorbed dose to water (1.0024) and air kerma (1.0028).

**Table 9. Comparison of  $N_{Dw}/N_K$  ratios at the ARPANSA and the BIPM**

Laboratory	Transfer chamber	$N_{Dw}/$ (Gy $\mu\text{C}^{-1}$ )	$N_K /$ (Gy $\mu\text{C}^{-1}$ )	$N_{Dw}/N_K$
ARPANSA	070	102.27	93.86	1.0896
	328	103.07	94.62	1.0893
BIPM	070	102.01	93.59	1.0899
	328	102.84	94.38	1.0896

## 5. Conclusion

The ratio of the ARPANSA and BIPM primary standard determinations of absorbed dose to water is 1.0024, with a standard uncertainty of 0.0029. The result will be used as the basis for an entry to the BIPM key comparison database and the determination of degrees of equivalence between the ten national metrology institutes (NMIs) which have finalized such comparisons. The standard uncertainty of the distribution of the results of the BIPM comparisons for these ten NMIs, shown in Figure 1 is  $2.5 \times 10^{-3}$ .



## Acknowledgements

We would like to thank L H Kotler (ARPANSA) for modelling the ARPANSA  $^{60}\text{Co}$  source and for the initial Monte-Carlo simulation of the spectrum, and M. Boutillon and J. Miles for their helpful improvements to the text.

## References

- [1] Huntley R B, Boas J F and Van der Gaast, H (1998) The 1997 determination of the Australian standards of exposure and absorbed dose at  $^{60}\text{Co}$ , *ARL/TR 126*, ISSN 0157-1400ARL, Victoria, Australia, 60 pages.
- [2] Huntley R B, Wise K N and Boas J F (2000) The Australian Standard of Absorbed Dose, Proceedings of the NPL Calorimetry Workshop, 8-10 December 1999, in press.
- [3] Boutillon M and Perroche A-M (1993) Ionometric determination of absorbed dose to water for cobalt-60 gamma rays, *Phys. Med. Biol.* **38** 439-454.

- [4] BIPM (1979) Comparaisons d'étalons de dose absorbée, *BIPM Comité Consultatif pour les Etalons de Mesure des Rayonnements Ionisants, Section (I)* vol 4 (Paris/ Offilib) p RI(6).
- [5] Wise K N (2000) Monte Carlo methods used to develop the Australian absorbed dose standard, *ARPANSA Technical Report ARPANSA/TR* (in preparation).
- [6] Burns J E and Dale J W G (1990) Conversion of absorbed dose calibration from graphite into water, *NPL Report RSA (EXT) 7* April 1990 Teddington U.K., 188 pages.
- [7] Burns J E (1994) Absorbed dose calibrations in high energy photon beams at the National Physical Laboratory: conversion procedure, *Phys. Med. Biol.* **39** 1555-1575.
- [8] Domen S R and Lamperti P J (1974) A heat-loss compensated calorimeter: theory, design and performance, *J. Res. NBS* **78A** 595-610.
- [9] Witzani J, Duftschmid K E, Strachotinsky Ch and Leitner, A (1984) A graphite absorbed dose calorimeter in the quasi-isothermal mode of operation, *Metrologia* **20** 73-79.
- [10] IAEA (1991), X- and gamma-ray standards for detector calibration, *IAEA-TEC-DOC-619*, 157 pages.
- [11] Pruitt J S and Loevinger R (1982) The photon-fluence scaling theorem for Compton scattered radiation, *Med. Phys.* **9** 176-179.
- [12] Higgins P D, Attix F H, Hubbell J H, Seltzer S M, Berger M J and Sibata C H (1992) Mass energy-transfer and mass energy-absorption coefficients, including in-flight positron annihilation for photon energies 1 keV to 100 MeV, *NIST Report NISTIR-4812*, Gaithersburg MD, 69 pages.
- [13] Boutillon M (1996) Measurement conditions used for the calibration of ionization chambers at the BIPM, *Rapport BIPM-96/1*, 19 pages.
- [14] BJR/IPEMB (1996) Central axis depth dose data for use in radiotherapy: *Brit. J. Radiol. Suppl.* **25**, 188 pages.
- [15] Allisy-Roberts P J, Boutillon M, Boas J F and Huntley R B (1998) Comparison of the air kerma standards of the ARPANSA and the BIPM for  $^{60}\text{Co}$   $\gamma$  rays, *Rapport BIPM-98/4*, 10 pages.

(October 2000)